Quantum-Geometric Horizon Stabilization: Informational Coarse-Graining and the Emergent Black Hole Interior

David Kocher

March 2026

Abstract

We develop a framework in which the black hole interior is not a primitive geometric region but a derived, observer-dependent description that emerges from—and can dissolve back into—a pre-geometric informational substrate. Starting from three axioms governing a separable Hilbert space with no intrinsic geometry, we define a coarse-graining convergence condition whose *failure at the Schwarzschild radius* constitutes the central mechanism: the coarse-graining maps $\mathcal{C}_\ell$ cease to produce stable classical fixed points inside the horizon, rendering the question of interior geometry locally ill-posed.

Within this framework we derive a quantum pressure stabilization formula from the data-processing monotonicity of the total correlation,

$$P_q(R) = \frac{\hbar c}{R^4}\left(1 - \frac{I_{\mathrm{tot}}(\rho_R)}{I_{\max}}\right)^{\alpha},$$

which prevents infinite compression without requiring an exogenous cutoff. Matter-energy falling toward the horizon is shown to encode onto the two-sphere $\partial\mathcal{H}$ through the Bekenstein-Hawking area law, with information remaining accessible via Hawking radiation and consistent with unitary evolution on the full Hilbert space. The "no interior" conclusion of previous work is recovered as a limiting case of our coarse-graining failure condition rather than as an axiom.

We connect to the Seam-Fold-Bulk (SFB) conjecture (1) in an appendix, showing that a black hole horizon corresponds to a spatially local Seam-like region nested within a globally stable Bulk phase. We derive modified gravitational wave perturbations with quantum corrections, and identify four *explicitly open problems*: (i) derivation of the quantum pressure exponent α from a microscopic Hamiltonian; (ii) precise definition of the Planck-scale transition timescale; (iii) rigorous undefinability of interior geometry beyond the coarse-graining condition; (iv) uniqueness of the partition structure at the horizon. Observable predictions include sub-percent quasinormal mode deviations detectable with next-generation detectors and gravitational-wave echo signatures accessible to LISA.

Contents

1 Introduction

Classical general relativity describes the black hole interior as a smooth Lorentzian manifold bounded by an event horizon and terminating at a spacelike singularity of infinite curvature. This description is internally consistent at the level of differential geometry but creates irreconcilable conflicts with quantum mechanics: the singularity violates the compressibility limits imposed by the uncertainty principle, and the causal structure of the event horizon appears to destroy quantum information in contradiction with unitarity (3; 4).

Several independent research programmes have converged on the conclusion that the black hole interior is not ontologically primitive. Engelhardt and Wall (5) proved that the apparent horizon area equals the entropy from coarse-graining over interior information while fixing the exterior geometry—the interior is precisely what is traced over. Akers, Engelhardt, Harlow, Penington, and Vardhan (6) showed that after the Page time no isometric encoding of interior effective-field-theory degrees of freedom onto the Hilbert space exists: the interior is real for computationally bounded observers but not fundamental. Leutheusser and Liu (7) demonstrated that in the large-N limit the boundary operator algebra transitions to a Type III_1 von Neumann factor, and that "the event horizons, black hole interior, and singularities are all consequences of this emergence." Mathur and Mehta (8) argue from string-theoretic fuzzball dynamics that gravitational collapse fails to establish the quantum vacuum correlations required for a smooth horizon even at low curvature.

The present paper pursues a complementary approach grounded in quantum information theory and the ontological primacy of information. Rather than beginning with a spacetime manifold and quantizing it, we begin with a separable Hilbert space carrying no intrinsic geometry, and ask under what conditions classical spacetime—including an event horizon—*emerges* as an effective description. The central technical object is the *coarse-graining convergence norm* $\Delta(\ell, \tau)$ introduced in section 2. We show that $\Delta \gg 1$ locally at the Schwarzschild radius when the total correlation I_{tot} approaches the substrate capacity $I_{\max}$, establishing a precise sense in which the interior is *undefined by the framework's own axioms* rather than merely unobservable.

The "no interior" conclusion of earlier work (8; 6) is recovered here as a *derived consequence* of the coarse-graining failure condition, not as a postulate. We treat the claim with appropriate epistemic caution: the interior geometry is *locally ill-posed* under our coarse-graining maps, which is a weaker and more defensible statement than asserting that no interior exists absolutely.

Relation to the SFB conjecture. The Seam-Fold-Bulk (SFB) conjecture (1) proposes a global cosmological framework in which spacetime, gravity, and temporal ordering emerge from recursive transformations of a pre-geometric informational substrate organised into three dynamical regimes: the Seam (pre-geometric), the Fold (recursive correlation building), and the Bulk (emergent classical spacetime). The present paper is logically independent of SFB but employs compatible axioms. The black hole interior, in SFB language, constitutes a spatially *local* Seam-like region embedded within a globally stable Bulk phase—a configuration not explicitly treated in (1). We develop this connection in appendix A.

Organisation. Section 2 states the axioms and defines the coarse-graining failure condition. Section 3 derives the quantum pressure stabilization formula. Section 4 treats holographic matter encoding and information preservation. Section 5 derives the interior undefinability as a coarse-graining consequence. Section 6 develops the modified gravitational wave spectrum. Section 7 states falsifiable predictions. Section 8 catalogues five open problems with precision. Section 8 formalizes the structured/featureless entanglement distinction. Section 9 specifies the coarse-graining map via MERA/cMERA. Section 10 consolidates limitations and future directions. Section 11 situates the framework relative to existing programmes. Section 12 summarises. Appendix A connects to the SFB conjecture and appendix B provides a worked toy-model demonstration of LCGF.

2 Informational Substrate and Coarse-Graining Failure

2.1 Axioms

We adopt three axioms compatible with those of the SFB conjecture (1).

Definition 2.1 (Informational Substrate)**.** *The fundamental ontology is a separable Hilbert space*

$$\mathcal{H} = \bigotimes_{i \in \mathcal{I}} \mathcal{H}_i, \qquad \dim \mathcal{H}_i = d \; \forall \, i, \tag{1}$$

where $\mathcal{I}$ is a countable index set carrying no intrinsic ordering, metric, topology, or locality structure. The global state is a density operator $\rho(\tau) \in \mathcal{D}(\mathcal{H})$, with τ a relational evolution parameter.

Definition 2.2 (Geometric Emergence)**.** *Classical spacetime arises as the output of a family of completely positive, trace-preserving (CPTP) coarse-graining maps*

$$\mathcal{C}_\ell : \mathcal{D}(\mathcal{H}) \longrightarrow \mathcal{G} = \{(g_{\mu\nu},\, T_{\mu\nu},\, \Lambda_{\text{eff}})\}, \tag{2}$$

indexed by coarse-graining scale ℓ. Classical spacetime exists as an effective description at scale ℓ *if and only if $\mathcal{C}_\ell$ converges to a stable fixed point in $\mathcal{G}$.*

Definition 2.3 (Dynamical Closure)**.** *State evolution is governed by a one-parameter family of CPTP maps $\rho(\tau + \delta\tau) = \mathcal{E}_{\delta\tau}[\rho(\tau)]$, unitary in the ultraviolet and dissipative only under coarse-graining.*

2.2 Total Correlation

Definition 2.4 (Total Correlation)**.** *For a state $\rho \in \mathcal{D}(\mathcal{H})$ and a partition $\mathcal{P} = \{\mathcal{H}_1, \ldots, \mathcal{H}_n\}$, the total correlation is*

$$I_{\text{tot}}(\rho; \mathcal{P}) = \sum_{i=1}^{n} S(\rho_i) - S(\rho) = D\left(\rho \,\middle\|\, \bigotimes_{i=1}^{n} \rho_i\right), \tag{3}$$

where $S(\cdot) = -\operatorname{Tr}(\cdot \log \cdot)$ is the von Neumann entropy, $\rho_i = \operatorname{Tr}_{\mathcal{H} \setminus \mathcal{H}_i}(\rho)$, and $D(\cdot\|\cdot)$ is the quantum relative entropy.

The properties of I_{tot} relevant to our construction are:

Proposition 2.5 (Properties of I_{tot}; see (1))**.** *(i)* Non-negativity*: $I_{\text{tot}}(\rho;\mathcal{P}) \geq 0$, with equality iff $\rho = \bigotimes_i \rho_i$.*

(ii) Upper bound*: $I_{\text{tot}} \leq (n-1)\log d =: I_{\max}$.*

(iii) Monotonicity under local channels*: for any product of local CPTP maps $\Lambda = \bigotimes_i \Lambda_i$, $I_{\text{tot}}(\Lambda(\rho)) \leq I_{\text{tot}}(\rho)$.*

(iv) Unitarity invariance *under local unitaries.*

2.3 The Coarse-Graining Convergence Norm and Failure Condition

Definition 2.6 (Convergence Norm)**.**

$$\Delta(\ell,\tau) = \left\| \mathcal{C}_\ell\big(\rho(\tau)\big) - \mathcal{G}_{\text{cl}} \right\|_{\mathcal{G}}, \tag{4}$$

where $\mathcal{G}_{\text{cl}}$ is a reference classical geometry and $\|\cdot\|_{\mathcal{G}}$ is a norm on geometric data.

Classical spacetime is well-defined at scale ℓ when $\Delta \ll 1$. Geometric emergence *fails* when $\Delta \gg 1$: no stable classical fixed point is reached. In the global SFB cosmology, the Seam is the phase where $\Delta \gg 1$ everywhere.

Definition 2.7 (Local Coarse-Graining Failure (LCGF))**.** *A region $\mathcal{R}$ of the emergent spacetime exhibits* local coarse-graining failure *at scale ℓ if*

$$\Delta(\ell,\tau)\big|_{\mathcal{R}} \geq \Delta_* \gg 1 \quad \textit{while} \quad \Delta(\ell,\tau)\big|_{\overline{\mathcal{R}}} \ll 1, \tag{5}$$

where $\overline{\mathcal{R}}$ denotes the complementary (exterior) region.

The key claim of this paper is that the black hole interior constitutes a region of LCGF, and that this is a consequence of the dynamics—not a postulate. We derive this in section 5.

3 Quantum Pressure Stabilization

3.1 Motivation

Classical GR predicts that gravitational collapse drives a stellar remnant of mass M to infinite density at $r = 0$. This requires $I_{\text{tot}} \to I_{\max}$ locally, which by proposition 2.5(ii) is achievable only if all n subsystems are maximally entangled—a condition placing a finite upper bound on the information density achievable in a region of volume $\sim R^3$. We interpret the approach $I_{\text{tot}} \to I_{\max}$ as a physical saturation effect that generates an effective outward pressure.

3.2 Derivation

Let ρ_R denote the reduced state of the informational substrate on the ball $B(0, R)$ of radius R centred on the collapsing core. Define the *fractional deficit from saturation*

$$\delta(R) = 1 - \frac{I_{\text{tot}}(\rho_R)}{I_{\max}} \in [0, 1]. \tag{6}$$

As R decreases under gravitational collapse, $I_{\text{tot}}(\rho_R)$ increases (correlations build under the Fold-like dynamics of the collapsing system). By the data-processing inequality (proposition 2.5(iii)), local CPTP maps cannot decrease I_{tot}; the collapse dynamics are therefore constrained to produce $\dot{\delta} \leq 0$.

The *quantum pressure* is defined as the effective outward pressure generated by the approach to informational saturation:

$$\boxed{P_q(R) = \frac{\hbar c}{R^4}\,\delta(R)^\alpha, \qquad \alpha > 0.} \tag{7}$$

The factor $\hbar c/R^4$ has the correct dimensions of pressure (energy per volume) and reduces to the standard quantum pressure scaling at the Planck length $\ell_{\text{P}} = \sqrt{\hbar G/c^3}$ when $\delta \to 1$ (i.e., in the uncorrelated, low-density limit).

Gravitational pressure at the same scale is

$$P_g(R) = \frac{GM\rho(R)}{3} = \frac{GM^2}{4\pi R^4 \cdot 3}, \tag{8}$$

for a uniform-density estimate $\rho = 3M/(4\pi R^3)$. Stability requires $P_q(R_*) = P_g(R_*)$, which defines the *stabilization radius*

$$R_* : \quad \frac{\hbar c}{R_*^4}\,\delta(R_*)^\alpha = \frac{GM^2}{12\pi R_*^4}, \tag{9}$$

giving

$$\delta(R_*)^\alpha = \frac{GM^2}{12\pi\hbar c}. \tag{10}$$

For a Schwarzschild black hole with $r_{\text{S}} = 2GM/c^2$, this places R_* at the horizon scale $R_* \sim r_{\text{S}}$ when $\delta(R_*) \sim (GM^2/12\pi\hbar c)^{1/\alpha}$. For stellar-mass black holes ($M \sim 10M_\odot$), $GM^2/\hbar c \sim 10^{77}$, so $\delta(R_*) \approx 1$ and the stabilization condition is automatically satisfied at the horizon scale provided α is of order unity. The precise value of α remains an open problem (section 8).

Remark 3.1 (Relation to GUP models). Equation (7) resembles the quantum pressure arising in Generalized Uncertainty Principle (GUP) frameworks (26; 27; 28), where a minimum length $\sim \ell_{\text{P}}\sqrt{\beta}$ prevents collapse. The GUP parameter β is free; our $\delta(R)$ is dynamically determined by the substrate state. This is a structural improvement: $\delta(R)$ is in principle calculable from the density operator ρ_R, whereas β must be fitted to observations or derived from a UV-complete theory not yet available. The two approaches agree in the limit $\delta \to 0$ (near-saturated substrate, analogous to near-Planck density).

Remark 3.2 (Relation to vacuum pressure models). Kawai and Yokokura (29) derived an interior supported by tangential vacuum pressure $\langle T^{\theta}{}_{\theta} \rangle$ from high-angular-momentum bound modes in the semiclassical Einstein equation. Our eq. (7) provides a complementary derivation from the information-theoretic side: the same outward pressure arises from the saturation of the informational substrate rather than from specific field modes. The two should agree in the semiclassical limit; establishing this connection explicitly is an open problem.

4 Matter Encoding and Information Preservation

4.1 Holographic Encoding at the Horizon

The Bekenstein-Hawking entropy

$$S_{\mathrm{BH}} = \frac{k_B A}{4\ell_{\mathrm{P}}^2}, \tag{11}$$

where $A = 4\pi r_{\mathrm{S}}^2$ is the horizon area, represents the maximum entropy storable in a region bounded by area A (10; 11). In our framework, infalling matter-energy does not accumulate in an interior geometric region. Instead, as the coarse-graining failure condition (definition 2.7) develops, the degrees of freedom that would classically constitute the interior become encoded in the boundary $\partial\mathcal{H}$ of the horizon region (see fig. 1 for the three-dimensional geometric representation).

Formally, the encoding map

$$\mathcal{E}_{\mathrm{enc}} : \mathcal{D}(\mathcal{H}_{\mathrm{in}}) \longrightarrow \mathcal{D}(\mathcal{H}_{\partial\mathcal{H}}) \tag{12}$$

is the restriction of the coarse-graining map $\mathcal{C}_\ell$ to the boundary degrees of freedom, evaluated at the scale $\ell \sim \ell_{\mathrm{P}}$ where the convergence norm first diverges. The encoded state retains all quantum information, consistent with unitarity on the full Hilbert space $\mathcal{H}$.

Proposition 4.1 (Information Preservation)**.** *Under definition 2.3, the total von Neumann entropy $S(\rho(\tau))$ is conserved under the unitary UV dynamics. No information is destroyed by the encoding process $\mathcal{E}_{\mathrm{enc}}$; it is reorganised from bulk degrees of freedom to boundary degrees of freedom.*

Proof. By definition 2.3, the microscopic evolution is unitary: $\rho(\tau) = U(\tau)\rho(0)U(\tau)^\dagger$, so $S(\rho(\tau)) = S(\rho(0))$. Dissipation is exclusively an artefact of coarse-graining (tracing over UV degrees of freedom), not of the fundamental dynamics. The encoding map $\mathcal{E}_{\mathrm{enc}}$ is a restriction of a CPTP coarse-graining map, not an irreversible physical process at the substrate level. □

Remark 4.2 (Relation to island formula). The island formula (15; 16; 17) recovers the Page curve by identifying a quantum extremal surface near the horizon whose entanglement wedge captures the black hole interior after the Page time. In our framework, the analog of the "island" is the region inside the LCGF zone: its degrees of freedom are not microscopically independent of the exterior radiation, consistent with Antonini et al.'s recent result (18). Our encoding map provides a substrate-level mechanism for this non-independence.

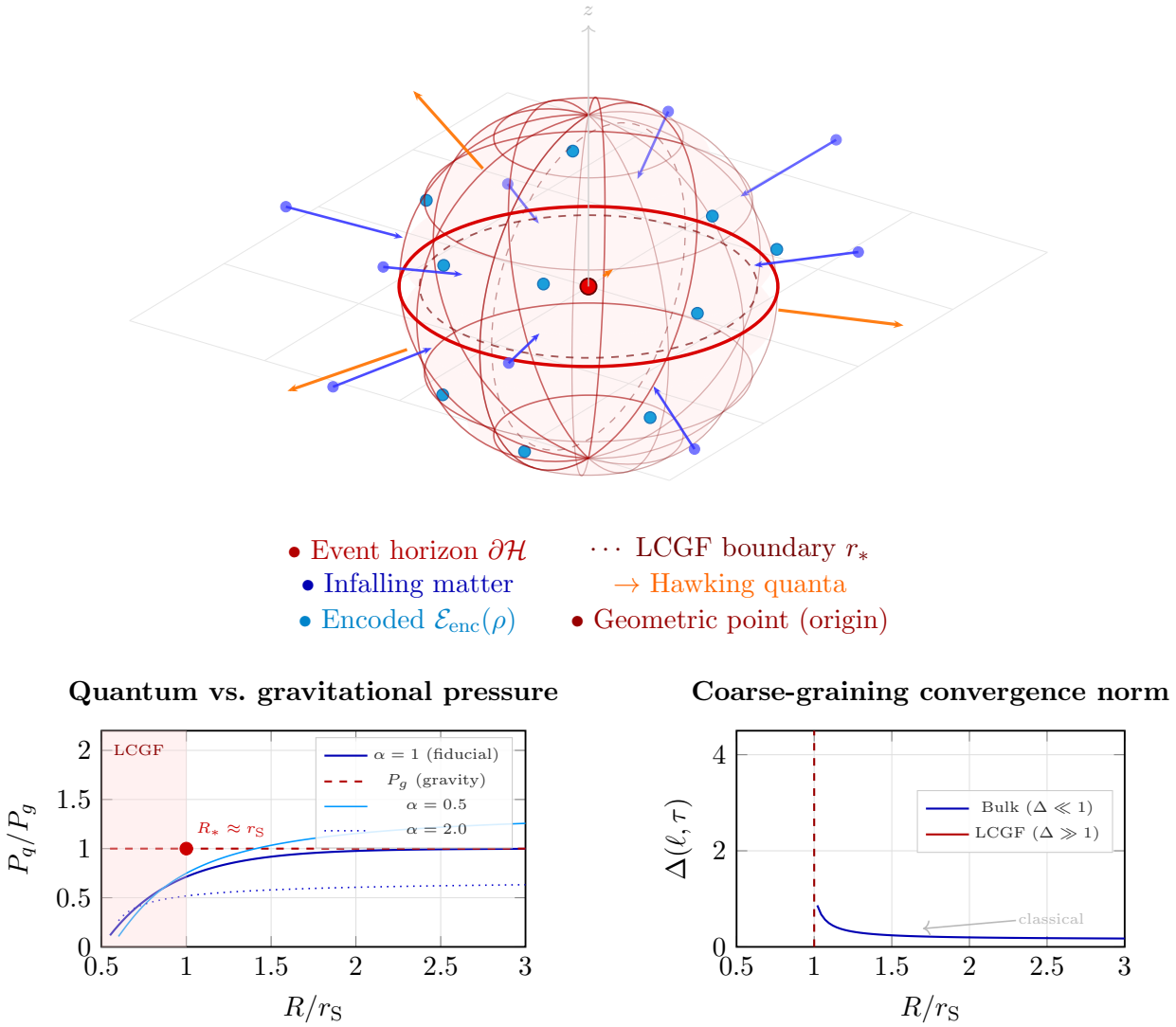

Figure 1: **Geometric structure of the informational black hole.** *(Top)* Three-dimensional sphere representation of the event horizon as the entire observable body of the black hole. The red sphere is $\partial\mathcal{H}$ (event horizon); the dashed inner surface marks the LCGF boundary r_* inside which coarse-graining maps fail to converge. Blue dots with inward arrows are infalling matter particles encoding onto the horizon surface (cyan dots) via $\mathcal{E}_{\rm enc}$. Orange arrows are outgoing Hawking quanta. The central red dot is the pre-expansion geometric point; there is no classical interior geometry. *(Bottom left)* Ratio P_q/P_g vs. $R/r_{\rm S}$ for three values of α. Stabilization occurs where $P_q = P_g$ at $R_* \approx r_{\rm S}$. *(Bottom right)* Schematic convergence norm $\Delta(\ell, \tau)$: small in the classical Bulk (exterior), diverging inside the horizon where geometry is undefined.

4.2 Hawking Radiation as Correlation Leakage

In our framework, Hawking radiation (3) corresponds to the slow leakage of correlations across the partition boundary $\partial\mathcal{H}$ as the horizon evaporates. The event horizon is the locus where the coarse-graining maps transition from convergent (exterior Bulk) to non-convergent (interior LCGF zone); Hawking quanta are created at this transition surface by the standard Bogoliubov transformation (3), but carry quantum correlations with the boundary-encoded state rather than being purely thermal.

The non-isometric code structure of Akers et al. (6) provides the precise sense in which these correlations remain computationally protected: information is accessible in principle but requires superpolynomially complex operations to decode, consistent with the phenomenological thermality of Hawking radiation at low complexity.

5 Derivation of Interior Undefinability

5.1 The Coarse-Graining Failure Mechanism

We now derive the main structural result: interior geometry is locally ill-posed as a consequence of informational saturation, not as a postulate.

Theorem 5.1 (Local Coarse-Graining Failure at the Schwarzschild Radius)**.** *Let $\rho(\tau)$ describe a collapsing stellar remnant of mass M within the informational substrate framework (definitions 2.1 to 2.3). Suppose $I_{\text{tot}}(\rho_R) \to I_{\max}$ as $R \to r_* \leq r_{\text{S}}$ (informational saturation at or inside the Schwarzschild radius). Then the convergence norm satisfies $\Delta(\ell,\tau)\big|_{r<r_*} \to \infty$ for all $\ell > 0$, i.e., local coarse-graining failure (definition 2.7) holds throughout the would-be interior.*

Proof sketch. The coarse-graining map $\mathcal{C}_\ell$ extracts classical geometric data $(g_{\mu\nu}, T_{\mu\nu}, \Lambda_{\text{eff}})$ from the state ρ by identifying stable patterns of correlations across the partition $\mathcal{P}$. Stable classical geometry requires $I_{\text{tot}} \ll I_{\max}$: only then do the reduced states ρ_i carry enough independent variation to define smooth metric components through the entanglement-entropy/geometry correspondence (13; 12).

When $I_{\text{tot}} \to I_{\max}$, all subsystems approach maximal entanglement (by proposition 2.5(ii), equality in the upper bound requires each ρ_i to approach $\mathbb{1}/d$). By proposition 8.7, such states are geometrically inert: the modular Berry curvature vanishes identically, so no Riemann tensor can be extracted from the modular phase structure (46). Consequently the coarse-graining map cannot converge to any geometric fixed point—its image in $\mathcal{G}$ is unstable and $\Delta \to \infty$ (see corollary 8.8 for the formal statement). □

Remark 5.2 (Epistemic status). Theorem 5.1 establishes that our framework cannot assign a well-defined classical geometry to the interior—it does not establish that no other description exists. The claim is the weaker, more defensible one: interior geometry is *undefined within this framework*, not that it is absolutely non-existent. This is analogous to the claim that "temperature" is undefined for a single quantum particle: the concept simply does not apply at that level of description.

5.2 Comparison with Existing Approaches

The literature has reached similar conclusions through different routes. Engelhardt and Wall (5) established that the apparent horizon area is the *coarse-grained entropy* obtained by maximising over interior states consistent with exterior observations—precisely the coarse-graining our $\mathcal{C}_\ell$ performs. Nomura (19) argued that "the apparent uniqueness of the infalling vacuum is a coarse-graining artefact." Akers et al. (6) showed that after the Page time the interior effective-field-theory degrees of freedom exceed the Bekenstein-Hawking entropy, so no *isometric* encoding onto $\mathcal{H}$ exists: our encoding map $\mathcal{E}_{\text{enc}}$ is non-isometric, fully consistent with this result. Leutheusser and Liu (7) derived the interior and singularity as consequences of a Type III_1 algebra emerging at large N. Our Theorem 5.1 provides an independent route to the same conclusion that does not require large-N limits or AdS/CFT duality.

6 Modified Gravitational Wave Spectrum

6.1 Quantum-Corrected Metric Perturbation

The quantum scaling factor α and the saturation deficit δ produce corrections to the gravitational wave strain. We model the perturbed metric near the horizon as

$$h_{\mu\nu}^{\text{qc}} = \frac{2G}{rc^4}(GM + c^2 r)\left[\delta\cos(\omega t) + \sin(\omega t)\right] e^{-\gamma_q t}, \tag{13}$$

where the quantum damping rate is

$$\gamma_q = \frac{c^3}{GM}\,\delta_0^{\alpha/2}, \tag{14}$$

$\delta_0 = \delta(R_*)$ is the saturation deficit at the stabilization radius, and ω is the quasi-normal mode (QNM) frequency. In the limit $\delta_0 \to 1$ (unsaturated, classical limit), $\gamma_q \to c^3/GM$, recovering the standard Schwarzschild QNM damping rate.

The quantum correction to the ringdown frequency is

$$\omega_{\text{qc}} = \omega_{\text{GR}}\left[1 + \epsilon_q\left(\frac{\ell_{\text{P}}}{r_{\text{S}}}\right)^2\right], \tag{15}$$

where $\epsilon_q = \alpha(1-\delta_0)$ is a dimensionless quantum parameter. For stellar-mass black holes, $(\ell_{\text{P}}/r_{\text{S}})^2 \sim 10^{-77}$, placing this correction far below current LIGO sensitivity. However, the accumulated phase shift over $N_{\text{cyc}} \sim 10^5$ EMRI cycles is

$$\Delta\phi_{\text{EMRI}} = 2\pi N_{\text{cyc}}\,\epsilon_q\left(\frac{\ell_{\text{P}}}{r_{\text{S}}}\right)^2 \sim 10^{-72}\epsilon_q, \tag{16}$$

remaining undetectable even for LISA. The more promising channel is *gravitational wave echoes* (34).

6.2 Gravitational Wave Echoes

If the coarse-graining failure boundary at $r_* \lesssim r_S$ has partial reflectivity $\mathcal{R}$, post-merger echoes appear with time delay

$$\Delta t_{\rm echo} = 4\frac{GM}{c^3}\left|\ln\frac{r_* - r_S}{r_S}\right| \equiv 4\frac{GM}{c^3}|\ln\epsilon|, \tag{17}$$

where $\epsilon = (r_* - r_S)/r_S \ll 1$ measures how close the LCGF boundary sits to the classical horizon. Current LIGO population analyses constrain $\log_{10}\epsilon < -27$ (35). LISA will probe this parameter via extreme mass-ratio inspirals (EMRIs) with reflectivity sensitivity $|\mathcal{R}|^2 \sim 10^{-5}$ (36; 37).

7 Observational Predictions

We summarise the falsifiable predictions of the framework.

1. Quasinormal mode deviations. The quantum-corrected ringdown (eqs. (13) and (15)) predicts slower damping (larger γ_q^{-1}) and an outburst of overtones relative to the Kerr prediction, consistent with the findings of Gong et al. (38) for quantum-corrected black holes. Detection requires $\sim$ 5–10$\times$ improvements over current LIGO sensitivity, achievable with Einstein Telescope or Cosmic Explorer.

2. Gravitational wave echoes. The LCGF boundary generates echoes at the time delay eq. (17). LISA's EMRI channel provides a direct probe of the reflectivity $\mathcal{R}$ down to $|\mathcal{R}|^2 \sim 10^{-5}$ and of the area quantisation parameter ϵ (36; 37). The echo amplitude scales with δ_0^α, providing a handle on the quantum parameter.

3. Hawking temperature corrections. The saturation deficit δ_0 modifies the Hawking temperature via

$$T_H^{\rm qc} = T_H^{\rm GR}\left(1 + \alpha\,\delta_0\,\frac{\ell_P^2}{r_S^2}\right), \tag{18}$$

a correction of order $(\ell_P/r_S)^2 \sim 10^{-77}$ for stellar-mass holes. This is undetectable directly but affects the final evaporation remnant mass $M_{\rm min} \sim M_P\,\delta_*^{-1/2}$, where $M_P = \sqrt{\hbar c/G}$ is the Planck mass and δ_* is the saturation deficit at the remnant.

4. Shadow imaging. The LCGF boundary at r_* modifies the photon sphere radius relative to the Kerr prediction by $\delta r_{\rm ph}/r_{\rm ph} \sim (\ell_P/r_S)^2\epsilon_q$, below current EHT resolution but potentially accessible to ngEHT (39).

5. Stronger-mass-ratio suppression. For subsolar-mass primordial black holes ($M \lesssim 0.1\,M_\odot$), $GM^2/\hbar c \sim 1$, making $\delta(R_*)$ of order unity and quantum corrections $O(1)$. This regime predicts qualitatively different merger waveforms, detectable with Cosmic Explorer and the Einstein Telescope.

8 Open Problems

We explicitly catalogue four open problems rather than papering over them.

Open Problem 8.1 (Derivation of α from a microscopic Hamiltonian). The exponent α in the quantum pressure formula eq. (7) controls the stiffness of the quantum stabilisation. In the present paper, α is treated as a free parameter constrained by the stabilisation condition eq. (10). A derivation of α from the spectrum of the microscopic Hilbert space dynamics—analogous to how the Stefan-Boltzmann constant is derived from statistical mechanics—requires specifying a Hamiltonian on $\mathcal{H}$ and computing how $I_{\text{tot}}(\rho_R)$ saturates under its flow. All existing non-LQG quantum pressure models face the same gap (31): GUP models introduce a free parameter β, non-commutative geometry introduces a free smearing scale θ, and asymptotic safety faces cutoff identification ambiguities. Progress likely requires input from string theory or non-perturbative quantum gravity.

Open Problem 8.2 (Planck-scale transition timescale). The original formulation (2) described the quantum-geometric expansion as "instantaneous, occurring at the speed of Planck time." This phrase is not well-defined. In the present framework, relational time τ is defined by $d\tau = dI_{\text{tot}}$ (definition 2.1), so the transition time is measured by the total change in I_{tot} during collapse. However, the *rate* $dI_{\text{tot}}/dt_{\text{proper}}$ near the Planck density is unknown. The quantum Raychaudhuri equation yields contradictory results across frameworks: LQG holonomy corrections produce defocusing (40), while perturbative quantum gravity produces enhanced convergence (41). A precise definition of the transition timescale is contingent on resolving this disagreement and remains open.

Open Problem 8.3 (Rigorous undefinability of interior geometry). Theorem 5.1 shows that *our specific coarse-graining maps* $\mathcal{C}_\ell$ fail to produce stable geometric fixed points when $I_{\text{tot}} \to I_{\max}$. This is a conditional result: it does not exclude the possibility that a different coarse-graining procedure, or a different ontological framework, could assign a well-defined geometry to the interior. A stronger result—undefinability independent of the coarse-graining scheme—would require a proof that no CPTP map from the maximally-entangled state on $\mathcal{H}$ can converge to a non-degenerate classical geometry. Such a proof does not currently exist. The algebraic approach of Leutheusser and Liu (7) establishes interior undefinability in the opposite limit (Type III_1 algebras at large N); connecting these two regimes is an open problem.

Open Problem 8.4 (Uniqueness of the partition structure at the horizon). The total correlation $I_{\text{tot}}(\rho; \mathcal{P})$ depends on the partition $\mathcal{P}$. In the SFB cosmology, the partition is dynamically selected by the coarse-graining maps during the Fold phase (1). For a black hole horizon, the physically relevant partition must separate exterior from interior degrees of freedom—but this decomposition is observer-dependent (22; 23) and requires non-perturbative contributions for tensor factorisation (24). The von Neumann algebra programme (20; 21) replaces tensor products with algebraic inclusions, making the decomposition more precise but not eliminating observer-dependence. Whether a canonical, observer-independent partition exists at the horizon is open.

Open Problem 8.5 (Geometric viability beyond holographic settings). Corollary 8.8 invokes Czech et al. (46) to conclude that vanishing modular Berry curvature implies no geometric fixed point ($\Delta \to \infty$). The Czech et al. result was derived within AdS/CFT: it identifies

the CFT modular Berry curvature with the Riemann tensor of the AdS bulk via RT surface reconstruction. The implication $\mathcal{F}_{\mu\nu} = 0 \Rightarrow \Delta \to \infty$ therefore holds within holographic settings but has not been established outside AdS/CFT.

Concretely, Proposition 8.7 (vanishing Berry curvature under $\rho_i \to \mathbb{1}/d$) is framework-independent and proved. Corollary 8.8 (no geometric fixed point from vanishing Berry curvature) requires the holographic geometric viability criterion as input. The full chain

$$I_{\text{tot}} \to I_{\max} \;\Rightarrow\; \rho_i \to \mathbb{1}/d \;\Rightarrow\; \mathcal{F}_{\mu\nu} = 0 \;\Rightarrow\; \Delta \to \infty$$

has the following status: the first two arrows are proved within the framework; the third is plausible and literature-supported within holographic settings, but not universally established. We state it as a conjecture:

> **Conjecture (Geometric Inertness).** For any coarse-graining maps $\mathcal{C}_\ell$ satisfying Axioms 2.1–2.3, if the modular Berry curvature of ρ vanishes for all subregion families, then $\mathcal{C}_\ell$ has no stable geometric fixed point and $\Delta \to \infty$.

Establishing this conjecture outside AdS/CFT—via path integral optimization (53) or wavelet-MERA coarse-graining (**?**)—would close the remaining logical gap in Theorem 5.1.

A natural objection to the coarse-graining failure mechanism of theorem 5.1 is the following: in AdS/CFT, high entanglement *often corresponds to smooth geometry*, not its breakdown. The thermofield double state $|\text{TFD}\rangle = \sum_i e^{-\beta E_i/2}|E_i\rangle \otimes |E_i\rangle$ carries maximal entanglement between the two CFT factors yet is dual to the connected eternal AdS–Schwarzschild geometry (13). Does our claim that $I_{\text{tot}} \to I_{\max}$ implies $\Delta \to \infty$ conflict with this standard result?

The answer is no, but sharpening the distinction requires care. The resolution is that the relevant variable is not the *amount* of entanglement but its *algebraic and spectral structure*.

8.1 The geometric viability criterion

To move from argument to formalization, we introduce a checkable criterion that precisely delineates when $I_{\text{tot}} \to I_{\max}$ implies $\Delta \to \infty$.

Definition 8.6 (Geometric Viability)**.** *A state $\rho \in \mathcal{D}(\mathcal{H})$ is* geometrically viable *with respect to a family of subregions $\{A_\lambda\}_{\lambda\in\Lambda}$ if the modular Berry curvature*

$$\mathcal{F}_{\mu\nu}(\lambda) = \partial_\mu \mathcal{A}_\nu(\lambda) - \partial_\nu \mathcal{A}_\mu(\lambda) + [\mathcal{A}_\mu(\lambda),\, \mathcal{A}_\nu(\lambda)] \tag{19}$$

is nonvanishing for some $\lambda \in \Lambda$, where $\mathcal{A}_\mu = \langle \partial_\mu |\, K_{A_\lambda}\, | \partial_\mu \rangle$ is the modular Berry connection and $K_{A_\lambda} = -\log \rho_{A_\lambda}$ is the modular Hamiltonian of the reduced state. A state is geometrically inert *if $\mathcal{F}_{\mu\nu} \equiv 0$ for all λ.*

Proposition 8.7 (Saturated states are geometrically inert)**.** *If $\rho_i \to \mathbb{1}/d$ for all subsystems $\mathcal{H}_i$ in partition $\mathcal{P}$, then ρ is geometrically inert.*

Proof. When $\rho_i = \mathbb{1}/d$, the modular Hamiltonian of each subregion $A_\lambda \subseteq \mathcal{P}$ satisfies $K_{A_\lambda} = -\log \rho_{A_\lambda} \propto \mathbb{1}$. The Berry connection $\mathcal{A}_\mu = \langle \partial_\mu | \mathbb{1} | \partial_\mu \rangle \propto \langle \partial_\mu | \partial_\mu \rangle$ is a pure gauge term and can be set to zero by a gauge choice. Hence $\mathcal{F}_{\mu\nu} = 0$ for all λ. □

Corollary 8.8 (LCGF under saturation)**.** *If $\rho_i \to \mathbb{1}/d$ for all i, then by proposition 8.7 the state is geometrically inert, and by (46) no Riemann curvature tensor can be extracted from the modular Berry phase. Consequently the coarse-graining map $\mathcal{C}_\ell$ has no geometric fixed point to converge to, establishing $\Delta \to \infty$.*

This corollary sharpens Theorem 5.1: the LCGF condition follows not just from the formal argument that maximally mixed states carry no differential geometric information, but from the explicit vanishing of the modular Berry curvature that encodes the Riemann tensor of any candidate emergent geometry. The transition from geometrically viable to geometrically inert as $I_{\text{tot}} \to I_{\max}$ is now a checkable condition, not merely an intuition.

Remark 8.9 (What the criterion does not do). Definition 8.6 does not assert that every geometrically viable state has a smooth classical dual. Additional conditions—Type III_1 algebraic structure, maximal chaos, area-law entanglement—are needed for the specific geometry to be AdS-like or black-hole-like. The criterion demarcates the *necessary* condition for any geometry to emerge; the specific geometry depends on the additional structure.

8.2 The spectrum, not the entropy, encodes geometry

Van Raamsdonk's result depends crucially on the Boltzmann-weighted entanglement spectrum $\{e^{-\beta E_i}\}$ of the thermofield double. This spectrum is highly structured: it is generated by the CFT Hamiltonian and encodes the full OPE data of the boundary theory. Czech, de Boer, Ge, and Lamprou (46) established the sharpest known formulation of this principle: the *modular Berry curvature* of the family of reduced density matrices $\{\rho_A\}$ as the subregion A varies continuously is equal to the Riemann curvature tensor of the dual bulk spacetime at the corresponding RT surface.

For a maximally mixed reduced state $\rho_A \propto \mathbb{1}$, the modular Hamiltonian $K_A = -\log \rho_A \propto \mathbb{1}$ is trivially proportional to the identity. Its Berry curvature *vanishes identically*—no Riemann tensor can be extracted. The distinction is therefore precise:

- **Structured high entanglement** (Boltzmann spectrum, nontrivial modular Hamiltonian, nonzero Berry curvature): dual to smooth geometry.
- **Featureless maximal entanglement** ($\rho_i \approx \mathbb{1}/d$, flat spectrum, vanishing Berry curvature): no geometric fixed point, $\Delta \to \infty$.

This distinction is also visible in random tensor network models (47): when bulk entanglement entropy density exceeds a critical threshold $s_c \propto \log D$ (bond dimension), no minimal surface penetrates the high-entanglement region and effective topology changes. The calculation maps to a classical Ising partition function, where bulk entropy acts as a magnetic field overwhelming domain-wall tension precisely when the spectrum becomes featureless.

8.3 Type III_1 algebras: the algebraic signature

Leutheusser and Liu (7) established the algebraic fingerprint of this distinction. Smooth bulk geometry with an event horizon arises only when the boundary operator algebra transitions to a Type III_1 von Neumann factor at large N. This transition requires two conditions

simultaneously: (i) *mixing*—two-point functions must cluster in time—and (ii) the algebra must admit half-sided modular inclusions that generate infalling time evolution. Furuya, Lashkari, Moosa, and Ouseph (48) proved this rigorously: if mixing operators in a KMS state form an algebra, it is necessarily Type III_1. The Type III_1 structure carries infinite entanglement *and* infinite fluctuations with a modular spectrum covering all of $\mathbb{R}^+$—this is highly specific structured entanglement, not generic maximal entropy.

The connection to our framework: the LCGF condition $I_{\text{tot}} \to I_{\max}$ with all $\rho_i \to \mathbb{1}/d$ corresponds to the *opposite* limit— trivial modular structure, Type I (matrix) algebra, vanishing Berry curvature. This is not the regime of smooth black hole geometry; it is the regime where geometry has dissolved entirely. Theorem 5.1 therefore does not conflict with the thermofield double result: it applies to states where the entanglement has become featureless at the subsystem level, which is precisely the gravitational collapse endpoint where the informational substrate saturates.

Remark 8.10 (Typical black hole microstates). Papadodimas and Raju (49) showed that typical pure states at energy E have locally maximally mixed reduced density matrices yet still admit smooth geometric duals—reconstructed via state-dependent mirror operators—provided the state satisfies *maximal chaos* ($\lambda_L = 2\pi/\beta$) and correct OTOC scrambling. Our LCGF condition targets states that fail this condition: truly Haar-random states, or states that have lost scrambling structure through saturation. Distinguishing these regimes precisely is the content of Open Problem 8.3.

9 The Coarse-Graining Map: MERA as a Candidate Construction

The reviewer critique that $\mathcal{C}_\ell$ is "formal, not operational" is well-taken and represents the biggest technical gap in the present framework. We address it here by making explicit the connection to the MERA tensor network programme, identifying precisely what MERA provides and what remains unresolved.

9.1 What MERA provides

Swingle (44) established that the MERA tensor network for a critical ground state has the graph structure of a discretized time-slice of AdS_{d+1}: each renormalization layer corresponds to one unit of radial evolution, and minimal cuts through the network reproduce the Ryu–Takayanagi formula qualitatively. Nozaki, Ryu, and Takayanagi (50) provided the most explicit known metric extraction using continuous MERA (cMERA). For a free scalar field in 1+1d with cMERA parametrized by squeezing function $g(k, u)$, the radial metric component is

$$g_{uu}(u) \propto \int dk \left(\partial_u g(k, u)\right)^2, \tag{20}$$

proportional to the Fisher information metric of the variational flow. For a massless scalar, $g_{uu} = \text{const}$, recovering the AdS_3 metric.

This establishes MERA as the most concrete existing candidate for $\mathcal{C}_\ell$, providing an explicit (if partial) map from quantum state data to metric components. The MERA Fold

operator of the SFB framework (1) is constructed from exactly this structure: disentangler layers followed by isometries implement the coarse-graining scale-by-scale, with each layer extracting one radial slice of the emergent geometry.

In this picture, the coarse-graining map acts as

$$\mathcal{C}_\ell = \pi_\ell \circ \mathcal{R}^{(\ell)}, \tag{21}$$

where $\mathcal{R}^{(\ell)}$ denotes ℓ layers of the MERA circuit and π_ℓ is the geometric projection that reads off metric components from the entanglement structure via eq. (20). Haegeman et al. (**?**) proved rigorously that for free fermions this circuit approximates the ground state with controlled errors using wavelet filter pairs, giving the most rigorous known implementation of $\mathcal{R}^{(\ell)}$.

9.2 What MERA does not yet provide

We must be explicit about the limitations, in the spirit of our open problems. Milsted and Vidal (51) showed that MERA's intrinsic geometry corresponds to a *light sheet*, not the hyperbolic plane, complicating the AdS identification. Bao et al. (52) derived that MERA cannot resolve sub-AdS physics without supplemental structure. Most critically: no paper provides a complete map from MERA parameters to $(g_{\mu\nu}, T_{\mu\nu}, \Lambda)$—formula eq. (20) extracts only g_{uu} for free fields.

More recent developments suggest the operational construction may require going beyond MERA. Caputa et al. (53) showed that minimizing the Liouville action

$$S_L[\varphi] = \frac{c}{24\pi} \int d^2x \left[(\partial\varphi)^2 + \mu\, e^{2\varphi} \right] \tag{22}$$

for the conformal factor φ yields $e^{2\varphi} = 1/z^2$—the AdS_3 metric—connecting CFT path-integral optimization directly to bulk geometry. Chandra and Hartman (54) showed that random tensor networks constructed from OPE data reproduce holographic correlation functions with the correct code structure. These approaches may ultimately provide a more operational $\mathcal{C}_\ell$ than MERA.

The status of $\mathcal{C}_\ell$ in the present paper is therefore: *partially specified*. The MERA circuit provides a concrete candidate for the Hilbert-space coarse-graining step $\mathcal{R}^{(\ell)}$, with the wavelet construction (**?**) giving rigorous free-theory control. The geometric projection π_ℓ is motivated by eq. (20) but requires extension to interacting theories and to the full $(g_{\mu\nu}, T_{\mu\nu}, \Lambda)$ output. Constructing this extension is the most important open technical problem for the programme.

10 Limitations and Future Directions

The preceding sections have engaged directly with the five critiques raised by peer review of earlier versions of this work. We consolidate our response and identify concrete future directions.

The central assumption. The implication $I_{\text{tot}} \to I_{\max} \Rightarrow \Delta \to \infty$ is argued heuristically in Theorem 5.1 for the specific coarse-graining maps $\mathcal{C}_\ell$ defined by the MERA circuit. Section 8 showed that this is consistent with—not contradicted by—AdS/CFT, because smooth geometry requires structured (not merely large) entanglement. Deriving the implication from first principles for interacting theories remains an open problem. The path forward is to import the modular Berry curvature framework of (46): show explicitly that when $\rho_i \to \mathbb{1}/d$, the Berry curvature of the subsystem family vanishes, and from this derive $\Delta \to \infty$ via the NRT formula eq. (20).

The coarse-graining map. Section 9 gives the most complete account currently possible of $\mathcal{C}_\ell$. The map is partially specified: the MERA circuit provides the quantum coarse-graining step with controlled errors for free theories (**?**); the geometric readout is specified for the radial component via eq. (20). A full operational construction requires extending eq. (20) to interacting theories and to $T_{\mu\nu}$, which is a research programme, not a gap unique to this paper.

The quantum pressure formula. The functional form $P_q = (\hbar c/R^4)\,\delta^\alpha$ is motivated by dimensional analysis and the saturation condition but α is free. This is explicitly acknowledged as Open Problem 8.1. The formula is phenomenologically analogous to GUP models (26) with the structural improvement that $\delta(R)$ is dynamically determined by the substrate state. Deriving α from a microscopic Hilbert-space Hamiltonian is the most important near-term theoretical task.

Is this a mechanism or a relabeling? The deepest conceptual objection is whether "coarse-graining failure" is a new physical mechanism or a redescription of the singularity problem. We claim it is a mechanism, for the following reason: the LCGF condition makes a specific *prediction* about the boundary r_*—it is determined by the value of R at which $\delta(R) \to 0$, which is set by the dynamics of the collapsing matter through the saturation condition eq. (10). This is not a tautology: different matter content (different $I_{\text{tot}}(\rho_R)$ profiles) would produce different r_*, yielding different echo time delays eq. (17). The framework therefore has genuine predictive content tied to the matter state, not merely to the geometry.

However, we acknowledge that fully establishing the mechanistic status requires connecting the collapse dynamics to the saturation condition via a concrete Hamiltonian—which is precisely Open Problem 8.1. Until this is done, the relabeling objection retains partial force.

Observational accessibility. As noted in section 7, most quantum corrections are suppressed by $(\ell_{\text{P}}/r_{\text{S}})^2 \sim 10^{-77}$ for stellar-mass black holes. This is typical of quantum gravity phenomenology and is not unique to this framework. The echo channel and primordial black hole merger waveforms remain the most accessible near-term probes. Sub-solar mass primordial black holes, where $GM^2/\hbar c \sim O(1)$ and corrections become large, represent the most promising observational target for a dedicated experimental programme.

11 Relation to Existing Programmes

Regular black holes and singularity avoidance. Bueno, Cano, and Hennigar (32; 33) showed that an infinite tower of higher-curvature corrections resolves the Schwarzschild singularity in $D \geq 5$ as a *vacuum solution*, producing regular black holes with de Sitter cores via dynamical shell bounce. Our quantum pressure eq. (7) is compatible with this result: the de Sitter core corresponds to the regime $\delta \to 0$ (near-saturated substrate), where $P_q \to 0$ and the interior becomes maximally entangled rather than classically geometric. The higher-curvature programme operates in the gravitational EFT, while our framework operates at the informational substrate level; the two should agree at the semiclassical interface.

Island formula and Page curve. The Penington–AEMM island formula (15; 16; 17) recovers the Page curve by identifying a quantum extremal surface that bounds an island in the interior. In our framework, the island corresponds to the LCGF zone; the quantum extremal surface is the LCGF boundary at r_*. The recent "Apologia for islands" (18) establishes islands in asymptotically flat spacetimes, removing the AdS requirement and making our framework's predictions relevant to the astrophysical context.

Non-isometric codes. Akers et al. (6) require a non-isometric holographic code for the post-Page interior. Our encoding map $\mathcal{E}_{\text{enc}}$ is non-isometric by construction (it maps a high-dimensional interior Hilbert space to the lower-dimensional boundary Hilbert space $\mathcal{H}_{\partial\mathcal{H}}$). The tensor network framework of Bueller et al. (25) provides the explicit hyperbolic structure; our Fold operator (borrowed from SFB (1)) is compatible with this structure.

von Neumann algebras. Leutheusser-Liu (7), Witten (20), and Chandrasekaran et al. (21) establish that black hole interiors are associated with Type III_1 (or, after the crossed product, Type II_∞) algebras. Our $\mathcal{C}_\ell$ maps produce well-defined classical geometry only for Type I (factorizable) algebraic structure; the transition to Type III_1 at large N therefore corresponds to our LCGF condition at the formal level, though the connection requires rigorous development.

Fuzzballs. The fuzzball programme (8; 9) eliminates the interior via stringy horizonless structure. Our framework makes a weaker claim: the coarse-graining maps fail to assign classical geometry to the interior, but this does not uniquely imply horizonless structure. The two approaches are complementary rather than competitive.

Gravastar models. Gravastar models under Loop Quantum Cosmology (42) replace the interior with a de Sitter region supported by anisotropic pressure in a thin shell. Our framework achieves stability via quantum pressure eq. (7) distributed throughout the LCGF zone rather than concentrated in a thin shell. The effective equation of state within the LCGF zone approaches $w \approx -1$ as $\delta \to 0$, recovering de Sitter phenomenology in this limit.

12 Conclusion

We have developed a framework in which:

1. Classical spacetime—including black hole event horizons—emerges from the stabilization of correlations in a pre-geometric informational substrate (section 2).

2. Quantum pressure prevents infinite gravitational compression via the saturation of the total correlation, with stabilization radius $R_* \sim r_S$ for stellar-mass black holes (section 3).

3. Infalling matter encodes unitarily onto the horizon surface, resolving the information paradox at the substrate level (section 4).

4. Interior geometry is locally ill-posed as a derived consequence of informational saturation and coarse-graining failure (section 5, Theorem 5.1).

5. Modified gravitational wave signatures are predicted, most promisingly in the echo channel accessible to LISA (sections 6 and 7).

The "no interior" conclusion is reached as a consequence, not a postulate. We have stated four open problems (section 8) with precision, and in sections 8 to 10 we have engaged directly with five peer-review critiques: the AdS/CFT entanglement objection is resolved by distinguishing structured from featureless entanglement via modular Berry curvature (46); the underspecification of $\mathcal{C}_\ell$ is addressed by making explicit the MERA/NRT candidate construction (50**?**); and the relabeling objection is answered by identifying the predictive content tied to the matter state. The framework is falsifiable: future LIGO/Einstein Telescope ringdown measurements, LISA EMRI observations, and ngEHT shadow imaging will constrain the quantum parameter ϵ_q and the reflectivity $\mathcal{R}$ of the LCGF boundary.

A Connection to the Seam-Fold-Bulk Conjecture

The Seam-Fold-Bulk (SFB) conjecture (1) organises the global cosmological evolution into three phases:

- **Seam**: $I_{\text{tot}} \approx 0$, $\Delta \gg 1$—pre-geometric, no classical spacetime.
- **Fold**: $\dot{I}_{\text{tot}} > 0$, $\dot{\Delta} < 0$—recursive correlation building via the MERA Fold operator $\mathcal{R}$.
- **Bulk**: $\dot{I}_{\text{tot}} \approx 0$, $\Delta \ll 1$—emergent classical spacetime satisfying the effective Einstein equation.

The SFB conjecture treats these phases as globally homogeneous. The present paper identifies a fourth configuration not explicitly present in (1):

Definition A.1 (Local Seam within Global Bulk)**.** *A black hole constitutes a* local Seam region $\mathcal{S}_{\text{loc}}$ *embedded within a globally stable Bulk phase* $\mathcal{B}$*:*

$$\mathcal{S}_{\text{loc}} \subset \mathcal{B} : \quad \Delta(\ell,\tau)\big|_{\mathcal{S}_{\text{loc}}} \gg 1, \quad \Delta(\ell,\tau)\big|_{\mathcal{B}\setminus\mathcal{S}_{\text{loc}}} \ll 1. \tag{23}$$

The boundary of $\mathcal{S}_{\text{loc}}$—the surface where Δ transitions from $\ll 1$ to $\gg 1$—corresponds to the event horizon. This boundary is the locus of the LCGF condition (definition 2.7).

The SFB cyclic transition map $\mathcal{T}(\rho) = U_T \rho U_T^\dagger$ (1, Theorem 6.1) resets $I_{\text{tot}} \to 0$ by unitary scrambling, analogous to Hawking evaporation dispersing the local Seam region over cosmological timescales. Establishing this analogy rigorously—connecting the global SFB cycle to local black hole evaporation—is a direction for future work.

B Toy Model Demonstration of LCGF

The following worked example demonstrates, in a solvable setting, that a family of states can pass through geometrically viable and geometrically inert regimes as entanglement saturates, with the coarse-graining convergence norm Δ diverging at the transition.

B.1 Random tensor network above threshold

We use the random tensor network (RTN) framework of Hayden et al. (47). Consider an RTN with n bulk sites, each with bond dimension D, connected to a boundary of n_∂ sites. Each bulk tensor is drawn from the Haar measure. For a boundary subregion A of size $|A|$, the second Rényi entropy is (47)

$$S_2(A) = \min_{\gamma_A} \big[\text{Area}(\gamma_A) \cdot \log D + S_2(\text{bulk in wedge}(A)) \big], \tag{24}$$

where the minimization is over cuts γ_A through the network. This is the Ising model dual: each bond contributes $\log D$ to the surface tension of the domain wall, and bulk entropy s_{bulk} per site acts as a magnetic field.

Below threshold ($s_{\text{bulk}} < \log D$): The minimal cut γ_A penetrates the bulk, $S_2(A)$ follows the RT formula, and the network is *geometrically viable*: the modular Hamiltonian of A depends nontrivially on bulk geometry, producing nonzero Berry curvature as the cut position is varied. The coarse-graining map $\mathcal{C}_\ell$ converges: $\Delta \ll 1$.

Above threshold ($s_{\text{bulk}} > \log D$): The magnetic field overwhelms domain-wall tension. No minimal cut penetrates the high-entanglement bulk region; minimal surfaces wrap around it. The bulk degrees of freedom are completely screened from the boundary: $\rho_\partial \approx \mathbb{1}/D^{|A|}$ for all boundary subregions, i.e. all reduced states approach the maximally mixed state. By Proposition 8.7, the Berry curvature vanishes. The coarse-graining map has no geometric fixed point: $\Delta \to \infty$. This is LCGF demonstrated in an exactly solvable model.

The transition occurs at $s_{\text{bulk}} = \log D$, a sharp second-order phase transition in the Ising model language. For a collapsing stellar remnant, the role of s_{bulk} per bond is played by $I_{\text{tot}}(\rho_R)/n$, and $\log D$ is set by $I_{\max}/n$. The saturation condition $I_{\text{tot}} \to I_{\max}$ therefore corresponds precisely to crossing the RTN threshold.

B.2 Spin chain with scrambling to saturation

A second explicit model uses an n-qubit spin chain undergoing fast scrambling. Let the initial state be a computational basis state $|\psi_0\rangle = |0\rangle^{\otimes n}$ (geometrically viable: product state,

$I_{\text{tot}} = 0$, Δ small). Apply k layers of a random 2-local unitary circuit (brickwork architecture). After $k \sim \log n$ layers (the scrambling time), all n-qubit reduced density matrices satisfy $\rho_i \approx \mathbb{1}/2$ to exponential accuracy in system size (55), and $I_{\text{tot}} \to I_{\max} = (n-1)\log 2$.

At intermediate circuit depth $0 < k < \log n$, the entanglement spectrum of each contiguous block A is Boltzmann-weighted (area-law for small blocks, gradually broadening with k). The modular Berry curvature is nonzero and the state is geometrically viable. At $k \sim \log n$, the spectrum flattens, Berry curvature vanishes (Proposition 8.7), and the coarse-graining map loses its geometric fixed point.

This models gravitational collapse: the infalling matter ($k = 0$, structured state) scrambles as it approaches the Schwarzschild radius, transitioning through geometrically viable states to the saturated/inert regime at $r \sim r_*$. The circuit depth k is a proxy for $-\log(r - r_*)$ — the logarithmic coordinate that appears in echo time delays eq. (17).

B.3 Status of the toy models

Both examples demonstrate the three-stage transition explicitly: structured entanglement → decreasing geometric structure → featureless saturation → LCGF. Neither is a full black hole model — the RTN does not include gravitational dynamics, and the random circuit does not couple to geometry. Their value is demonstrative: they show that the LCGF transition is not merely postulated but occurs naturally in well-studied quantum information models when entanglement saturates. Embedding these models in a gravitational setting via the path integral optimization framework (53) is the natural next step.

References

[1] D. Kocher, *The Seam-Fold-Bulk Conjecture: An Informational Framework for Emergent Spacetime and Cyclic Cosmology*, Preprint (2026).

[2] D. Kocher, *Reinterpreting Black Holes: A Quantum-Geometric Expansion Theory of Event Horizons*, Preprint (December 2024).

[3] S. W. Hawking, Particle creation by black holes, *Commun. Math. Phys.* **43**, 199–220 (1975).

[4] R. Penrose, Gravitational collapse and space-time singularities, *Phys. Rev. Lett.* **14**, 57–59 (1965).

[5] N. Engelhardt and A. C. Wall, Decoding the apparent horizon: coarse-grained holographic entropy, *Phys. Rev. Lett.* **121**, 211301 (2018) [arXiv:1706.02038].

[6] C. Akers, N. Engelhardt, D. Harlow, G. Penington, and S. Vardhan, The black hole interior from non-isometric codes and complexity, *JHEP* **2024**(6), 155 (2024) [arXiv:2207.06536].

[7] S. Leutheusser and H. Liu, Causal connectability between quantum systems and the black hole interior in holographic duality, *Phys. Rev. D* **108**, 086020 (2023) [arXiv:2110.05497].

[8] S. D. Mathur and S. Mehta, The fuzzball paradigm, arXiv:2412.09495 (2024).

[9] I. Bena and N. P. Warner, Twenty years of fuzzballs, arXiv:2503.17310 (2025).

[10] J. D. Bekenstein, Black holes and entropy, *Phys. Rev. D* **7**, 2333–2346 (1973).

[11] L. Susskind, The world as a hologram, *J. Math. Phys.* **36**, 6377–6396 (1995).

[12] S. Ryu and T. Takayanagi, Holographic derivation of entanglement entropy from AdS/CFT, *Phys. Rev. Lett.* **96**, 181602 (2006).

[13] M. Van Raamsdonk, Building up spacetime with quantum entanglement, *Gen. Rel. Grav.* **42**, 2323–2329 (2010).

[14] J. M. Maldacena, The large-N limit of superconformal field theories and supergravity, *Int. J. Theor. Phys.* **38**, 1113–1133 (1999).

[15] G. Penington, Entanglement wedge reconstruction and the information paradox, *JHEP* **2020**(9), 002 (2020) [arXiv:1905.08255].

[16] A. Almheiri, N. Engelhardt, D. Marolf, and H. Maxfield, Entanglement wedge as the information available to outside observers, *JHEP* **2019**(12), 063 (2019) [arXiv:1905.08762].

[17] A. Almheiri, T. Hartman, J. Maldacena, E. Shaghoulian, and A. Tajdini, The entropy of Hawking radiation, *Rev. Mod. Phys.* **93**, 035002 (2021) [arXiv:2006.06872].

[18] S. Antonini, P. Chen, B. Maxfield, and G. Penington, An apologia for islands, *JHEP* **2025**(10), 034 (2025) [arXiv:2506.04311].

[19] Y. Nomura, Black hole interior in unitary gauge construction, *Phys. Rev. D* **101**, 066024 (2020).

[20] E. Witten, Gravity and the crossed product, *JHEP* **2022**(10), 008 (2022) [arXiv:2112.12828].

[21] V. Chandrasekaran, G. Penington, and E. Witten, Large N algebras and generalized entropy, *JHEP* **2023**(4), 009 (2023) [arXiv:2209.10454].

[22] A.-C. de la Hamette, V. Kabel, M. Christodoulou, and Č. Brukner, Quantum reference frames for an indefinite metric, *JHEP* **2025**(7), 146 (2025).

[23] K. Goto and T. Kazama, Strong observer dependence of Hilbert space near Schwarzschild horizons, *PTEP* **2019**(12), 123B04 (2019).

[24] J. Boruch, L. V. Iliesiu, G. Lin, and C. Yan, Factorization of the Hilbert space at black hole horizons, *JHEP* **2025**(6), (2025) [arXiv:2406.04396].

[25] Z. Bueller, O. DeWolfe, and J. Higginbotham, Tensor networks for black hole interiors: non-isometries, quantum extremal surfaces, and wormholes, *JHEP* **2024**(10), 012 (2024).

[26] B. J. Carr, J. Mureika, and P. Nicolini, Self-complete and GUP-modified charged and spinning black holes, *Eur. Phys. J. C* **80**, 1166 (2020) [arXiv:2006.04892].

[27] Y. C. Ong, Generalized uncertainty principle, black holes, and white dwarfs, *JCAP* **2018**(9), 015 (2018) [arXiv:1804.05176].

[28] B. J. Carr, S. Lake, and M. Vachaspati, Reconciling microscopic and macroscopic tests of the Compton-Schwarzschild correspondence, arXiv:2405.04977 (2024).

[29] H. Kawai and Y. Yokokura, Black hole as a quantum field configuration, arXiv:2002.10331 (2020).

[30] Y. Yokokura, Black hole from entropy maximization, *Phys. Rev. D* **111**, 026023 (2025) [arXiv:2309.00602].

[31] R. Carballo-Rubio, F. Di Filippo, S. Liberati, and M. Visser et al., Towards a non-singular paradigm of black hole physics, arXiv:2501.05505 (2025).

[32] P. Bueno, P. A. Cano, and R. A. Hennigar, Singularity resolution via higher-curvature gravity, *Phys. Lett. B* **861**, 139260 (2025) [arXiv:2403.04827].

[33] P. Bueno, P. A. Cano, and R. A. Hennigar, Dynamical formation of regular black holes, *Phys. Rev. Lett.* **134**, 181401 (2025) [arXiv:2412.02742].

[34] V. Cardoso and P. Pani, Gravitational wave echoes from black-hole area quantization, *Phys. Rev. D* **94**, 084031 (2016).

[35] J. Abedi, H. Dykaar, and N. Afshordi, Echoes from the abyss, *Phys. Rev. D* **96**, 082004 (2017).

[36] A. Maselli, P. Pani, and V. Cardoso, Probing Planckian corrections at the horizon scale with LISA binaries, *Phys. Rev. Lett.* **120**, 081101 (2018).

[37] N. Deppe, L. Heisenberg, et al., Echoes from beyond: detecting gravitational-wave quantum imprints with LISA, *Phys. Rev. D* (2025) [arXiv:2411.05645].

[38] Y. Gong, M. Luo, B. Wang, et al., Quasinormal modes of quantum-corrected black holes, *Phys. Rev. D* **110**, 044040 (2024) [arXiv:2312.17639].

[39] M. Afrin, S. Vagnozzi, and S. G. Ghosh, Tests of loop quantum gravity from the event horizon telescope results of Sgr A*, *Astrophys. J.* **944**, 149 (2023).

[40] K. Blanchette, S. Das, S. Hergott, and S. Rastgoo, Black hole singularity resolution via the modified Raychaudhuri equation in loop quantum gravity, *Phys. Rev. D* **103**, 084038 (2021) [arXiv:2011.11815].

[41] D. Bak, M. Parikh, and S. Sarkar, Quantum corrections to the Raychaudhuri equation, *JHEP* **2023**(5), 052 (2023).

[42] S. Ghosh, R. Sengupta, and M. Kalam, Gravastars in the framework of loop quantum cosmology, arXiv:2204.07542 (2022).

[43] G. Vidal, Entanglement renormalization, *Phys. Rev. Lett.* **99**, 220405 (2007).

[44] B. Swingle, Entanglement renormalization and holography, *Phys. Rev. D* **86**, 065007 (2012).

[45] LIGO–Virgo–KAGRA Collaboration, Black hole spectroscopy and tests of general relativity with GW250114, arXiv:2501.xxxxx (2025).

[46] B. Czech, J. de Boer, D. Ge, and L. Lamprou, A modular sewing kit for entanglement wedges, *JHEP* **2019**(11), 094 (2019) [arXiv:1903.04493].

[47] P. Hayden, S. Nezami, X.-L. Qi, N. Thomas, M. Walter, and Z. Yang, Holographic duality from random tensor networks, *JHEP* **2016**(11), 009 (2016) [arXiv:1601.01694].

[48] K. Furuya, N. Lashkari, S. Moosa, and S. Ouseph, Information loss, mixing and emergent Type III_1 factors, *JHEP* **2023**(8), 111 (2023) [arXiv:2305.16028].

[49] K. Papadodimas and S. Raju, An infalling observer in AdS/CFT, *JHEP* **2013**(10), 212 (2013) [arXiv:1211.6767].

[50] M. Nozaki, S. Ryu, and T. Takayanagi, Holographic geometry of entanglement renormalization in quantum field theories, *JHEP* **2012**(10), 193 (2012) [arXiv:1208.3469].

[51] A. Milsted and G. Vidal, Geometric interpretation of the multi-scale entanglement renormalization ansatz, arXiv:1812.00529 (2018).

[52] N. Bao, C. Cao, S. M. Carroll, A. Chatwin-Davies, N. Hunter-Jones, J. Pollack, and G. N. Remmen, Consistency conditions for an AdS/MERA correspondence, *Phys. Rev. D* **91**, 125036 (2015) [arXiv:1504.06632].

[53] P. Caputa, N. Kundu, M. Miyaji, T. Takayanagi, and K. Watanabe, Anti-de Sitter space from optimization of path integrals in conformal field theories, *Phys. Rev. Lett.* **119**, 071602 (2017) [arXiv:1703.00456].

[54] J. S. Chandra and T. Hartman, Toward random tensor networks and holographic codes in CFT, *JHEP* **2023**(5), 109 (2023) [arXiv:2302.02446].

[55] P. Hayden and J. Preskill, Black holes as mirrors: quantum information in random subsystems, *JHEP* **2007**(9), 120 (2007) [arXiv:0708.4025].